Hopfield neural network and pareto optimal algorithms for retrieving sea surface current from TanDEM-X data

Maged Marghany[1,2]

[1]Geography Section, Faculty of Humanities, Universiti Sains Malaysia, Penang
[2]Faculty Geospatial and Real Estate, Geomatica University College,Kuala Lumpur

magedupm@hotmail.com

Abstract . This is first work is done on the application of TanDEM-X data satellite data for the Malaysian coastal waters. This study aims at comparison between Hopfield neural network and Pareto optimal algorithms for modelling sea surface current using TanDEM-X satellite data. In fact, X-band data have a great potential for retrieving sea surface parameters such as sea surface current movement and ocean wave spectra. Therefore, TanDEM-X is the term of the satellite operation hovering the two satellites in a strictly controlled foundation with regular distances between 250 and 500 m. The study of ocean surface current is important for understanding the coastal water circulation. The set of TanDEM-X satellite data are examined by using Hopfield neural network algorithm. The sea surface current is retrieved based on the energy function. Therefore, the Pareto optimal algorithm is used to determine the optimal solution for nonlinearity problem which is raised due to the Doppler frequency shift impact. The study shows that the Pareto optimum resolution has highest performance than Hopfield neural network rule with lowest RMSE of ±0.08. Further, Pareto optimum resolution can verify the ocean surface current pattern variation on coastal water from TanDEMX data. Last, TanDEMX data reveals a superb guarantees for retrieving ocean surface current with X-band.

1. Introduction

Complexity of ocean nature needs standard instruments and procedures to comprehend. Despite advance technology of ocean in situ measurements, large ocean area cannot survey with effortless[1]. In reality, whether circumstances induce storms, which cause disasters in coastal zone that do not allow oceanographers and researchers to acquire timeless and effortless in situ measurements. Recently, researchers have shown an increased interest in ocean studies using remote sensing technology, which can image large-scale ocean area and provides precisely information on air-sea surface interactions [2-9]. Synthetic aperture radar (SAR) is recognized as the potential radar sensor for monitoring the dynamic ocean surface. One of an attention-grabbing topic is current flow that is needed short go back satellite cycle and high resolution. These will provide precisely data concerning current dynamic flow [10][12]. In fact, current is very important for ship navigation, fishing, waste matter substances transport and sediment transport [2][11]. Respectively optical and microwave sensors are enforced to monitor the current flows. Indeed, the ocean surface dynamic options of sea surface current is vital parameters for atmospheric-sea surface interactions. In this regard, the global climate change, marine pollution and coastal risky are preponderantly dominated by current speed and direction [12].

The measurements of ocean current from space relies on the electromagnetic signal. Truly, associate degree of an electromagnetic signal of optical and microwave reflects from the ocean carrying records concerning one among the first discernible quantities that are the colour, the beamy

temperature, the roughness, and also the height of the ocean [13]. The principal conception to retrieve the ocean surface current from SAR information is perform of the Doppler frequency shift theory [14]. Incidentally, the orbital quality of the ocean wave and surface current dynamic interactions will cause shifting of the radiolocation signal within the angle direction i.e. the flight direction that is thought because the Doppler frequency shift [11]. In truth, the surface current dynamic is virtual to the orbital movement and an antenna rotation of the synthetic aperture radar. Consequently, the Doppler frequency shift, reckon the SAR antenna angle of view that is virtual to the orbital mechanical phenomenon rotation [15]. Consequently, the connection between the ocean surface dynamic orbital movement and also the SAR satellite orbital motion would be nonlinear attributable to the Doppler influence [16]. In literature, there are many mathematical algorithms that are supported physical models to retrieve ocean surface current from SAR information. In other words, these algorithms area unit enforced to map the Doppler frequency spectra into the important ocean surface current speed. However, these techniques are restricted attributable to the nonlinear quality of ocean surface dynamic behaviours and radar signal [3]. In this regard, the Doppler rate has coarser resolution than radar cross section on the angle direction [17].

In this paper, we have a tendency to address the question of retrieving ocean surface current pattern from TanDEM-X data. This is often verified an exploitation of neural network technique. Hypotheses examined are: (i) Hopfield neural network based mostly multi-objective optimisation via Pareto dominance algorithmic rule is executed to TanDEM-X data; (ii) multi-objective optimisation via Pareto dominance is used as procedures for eliminating inherent speckle from TanDEM-X data; and (iii); the nonlinearity of the physicist frequency shift is reduced multi-objective optimisation via Pareto dominance.

The novelty of this work is to optimize the lapses occurring on retrieving sea surface current parameters from TanDEM-X satellite data. Hypotheses examined are: (i) Hopfield neural network based mostly multi-objective optimisation via Pareto dominance algorithmic rule is executed to TanDEM-X data; (ii) multi-objective optimisation via Pareto dominance is used as procedures for eliminating inherent speckle from TanDEM-X data; and (iii); the nonlinearity of the physicist frequency shift is reduced multi-objective optimisation via Pareto dominance.

2. Data Acquisitions

Two styles of knowledge area unit needed to retrieve sea surface current parameters: TanDEM-X of SAR; (ii) and therefore the real unaltered sea surface current measuring throughout TanDEM-X satellite overpassed.

2.1 TanDEM-X Data

Pair of Terra-SAR satellite data is acquired by the TanDEM-X satellite on May 6 2017. The first image was acquired 7:27:17 am while the second image acquired at 19:20:06 pm. The data are in spotlight mode with X-band and HH and VV polarization. These data are single look complex formatted data.

The TanDEM-X operational consequence involves the coordinated operation of 2 satellites flying in adjacent configuration. The alteration constraints for the formation are: (i) the orbits ascending nodes, (ii) the angle between the perigees, (iii) the orbit eccentricities and (iv) the phasing between the satellites. The observance of ocean currents is a vital facet of assessing climate changes. Space borne SAR along-track interferometry (ATI) has the promise to considerably contribute to the present field. It will offer large-area, world-wide surface current measurements. The matter of mapping relatively low velocities are often resolved by formations of SAR satellites that yield sufficiently sensitive ATI measurements [18]].

In this study, the Hopfield algorithm relies on the TanDEMX information. The TerraSAR-X and TanDEM-X satellites transmit identical SAR instruments working at 9.65 GHz frequency (X-band). Throughout some devoted operations, both satellites are placed associate exceedingly in a very special orbit configuration with a brief along track baseline providing a probability for current measurements. The data utilized in this study were uninheritable in stripmap (SM), bistatic (TS-X active / TD-X passive) mode and VV polarization [14][18].

2.2 In situ ocean wave measurement

Following Marghany [19] sea surface current speed and direction are collected by Aquadopp® 2MHz current meter (Figure 1). For the surface current knowledge acquisition, the Aquadopp® 2MHz current meter factory-made by Nortek AS (Figure1), Scandinavian country was used. The instrumentality could be a standalone instrumentation exploitation Doppler based mostly technology to measure surface currents at the deployment web site. The instrumentation is intended with intrinsically memory and internal battery pack wherever it may be designed to record and store information internally for self-deployment[19].

Figure 1. Aquadopp 2Mhz current meter deployment.

The Aquadopp® 2MHz current meter was deployed on coastal water of Teluk Kemang, Port Dickson, Malaysia on May 6 2017. (Figure 2). Two phases of data collection were carried out: (i) at 6:15 am to 8:15 am and (ii) at 6:15 pm to 8:15 pm. The surface current data was measured for intervals of 2 hours for both phases.

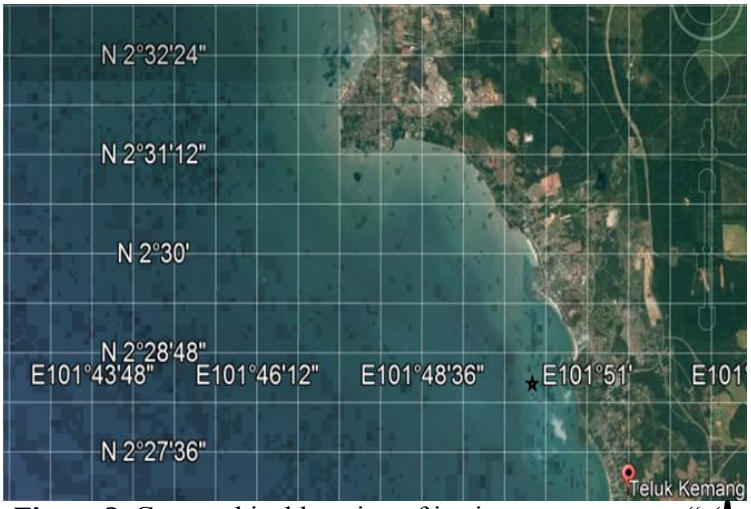

Figure 2. Geographical location of in situ measurements “

3. Algorithms

3.1 Hopfield Neural Network Algorithm

Marghany [19] has implemented Hopfield neural networks for RADARSAT-2 SAR data to retrieve sea surface current. This section has been retrieved from Marghany [11] work. Therefore, Hopfield

neural networks is used with TanDEM-X data. Consistent with Côté and Tatnall [20], Hopfield neural networks is considered as a promising method for determining a minimum of energy of function. For instance, motion analysis and object pattern recognitions might be coded into an energy function [21]. Furthermore, the actual physical constraint, heuristics, or prior knowledge of sea surface features, nonlinearity and the Doppler frequency shift [11] can be coded into the energy function.

A pattern, in the context of the *N* node Hopfield neural network is an *N*-dimensional vectors $V = (v_1, v_2, ...v_n)$ and $U = (u_1, u_2, ...u_n)$ from space $S = \{-1,1\}^N$. A special subset of S is set of exemplar $E = \{e^k : 1 \le k \le K\}$, .where $e^k = (e^k{}_1, e^k{}_2, ..., e^k{}_n)$ and k is exemplar pattern where $1 \le k \le K$ [19]. The Hopfield net associates a vector from S with an exemplar pattern in *E.* Following Marghany [19], Hopfield net is involved that $w_{ij} = w_{ji}$ and $w_{ii} = 0$. Succeeding, Cao and Wang, [20], the propagation rule τ_i which defines how neuron sates and weight combined as input to a neuron can be described by equation 1 as follows:

$$\tau_i = \sum_{j=1}^{N} f_t(j) w_{ij} \qquad (1)$$

The Hopfield algorithm has consisted of (i) assign weights to synaptic connections; (ii) initialize the net with unknown pattern; and (iii) iterate until convergence and continue features tracking (equation 2) [5]. First step of assign weight w_{ij} to synaptic connection can be achieved as understands:

$$w_{ij} = \begin{cases} \sum_{k=1}^{K} e_i^K e_j^K & \text{if} \quad i \ne j \\ 0 & i = j \end{cases} \qquad (2)$$

Hopfield neural network could be identified current pattern features by mathematical comparing to each other in order to build an energy function [19]. According to Côté and Tatnall [20] the difference function to determine the discriminations between different features f_i, f_j by a given equation 3 as follows:

$$diff(f_i, f_j) = G.\max\left|\max(\frac{l_i}{l_j}, \frac{l_j}{l_i}) - L'', 0\right| + H.\max[\min(\left|\theta_i - \theta_j\right|, 2\pi - \left|\theta_i - \theta_j\right| - \theta'', 0] + J.\max\left|dis_{ij} - dist'', \theta\right| \qquad (3)$$

where, L'' is curvature shape of current feature, dis_{ij} is the distance between sea surface current features f_i and f_j, and *G* and *H* and *J* are constants, and θ is an angle of orientation of local curve element. In addition, $dist''$ and θ'' are the minimum acceptable distance and the maximum acceptable rotation angle, respectively before energy function[19-21].

3.2 Pareto Algorithm

Following Atashkari et al., [22], the Multi-objective optimization (MOB) which is also termed the multi-criteria optimization or vector optimization. In this regard, it has been defined as finding a vector of decision variables satisfying constraints to give acceptable values to all objective functions. Generally, it can be mathematically defined as: find the vector $S^* = \left[S_1^*, S_2^*, ..., S_n^*\right]^T$ to optimize

$$F(S) = \left[f_1(S), f_2(S), ..., f_k(S)\right]^T, \qquad (4)$$

subject to *m* inequality constraints

$$g_i(S) \le 0 \quad , \quad i = 1 \text{ to } m \quad , \qquad (5)$$

and *p* equality constraints

$$h_j(S) = 0 \quad , \quad \text{j} = 1 \text{ to p}, \qquad (6)$$

where $S^* \in \Re^n$ is the vector of decision or design variables, and $F(S) \in \Re^k$ is the vector of objective functions which each of them be either minimized or maximized. However, without loss of generality, it is assumed that all objective functions are to be minimized.

A point $S^* \in \Omega$ (Ω is a feasible region in $\Re^n$ satisfying equations (4) and (6) is said to be Pareto optimal (minimal) with respect to the all $S \in \Omega$ if and only if $F(S^*) < F(S)$. Alternatively, it can be readily restated as $\forall i \in \{1,2,...,k\}, \forall S \in \Omega - \{S^*\} \quad f_i(S^*) \le f_i(S) \quad \wedge \quad \exists j \in \{1,2,...,k\}$: $f_j(S^*) < f_j(S)$.

In other words, the solution S^* is said to be Pareto optimal (minimal) of ocean current pattern if no other solution can be found to dominate S^* using the definition of Pareto dominance. For a given MOP, the Pareto front $\mathcal{PF}^*$ is a set of vector of objective functions which are obtained using the vectors of decision variables in the Pareto set $\mathcal{P}^*$, that is $\mathcal{PF}^* = \{F(S) = (f_1(S), f_2(S),...., f_k(S)) : S \in \mathcal{P}^*\}$. In other words, the Pareto front $\mathcal{PF}^*$ is a set of the vectors of objective functions mapped from $\mathcal{P}^*$ [19].

4. Results and Discussion

The sea surface current velocities are simulated and modelled from the TanDEM-X data spotlight with VV polarization. The simulation has been done along the range direction. The simulated velocity is taken across the location of The Aquadopp® 2MHz current meter (Figure 3). The test area is shown in Figure 1 which is inshore the coastal water of the Malacca Straits, Malaysia. Figure 4 shows TanDEM-X data cross section values increased with the increasing of the incidence angle where the backscatter value is raised to -10 dB. The second curve is the result of the Doppler shift frequency. The curve shows that the Doppler shift frequency values were fluctuated with value decreasing in the onshore 2km to 5 km. The frequency value in the nearshore area was extremely low with 0.1 m/s. The spectra peak of Doppler frequency is 0.04 with range frequency of -200 Hz. The average of the Doppler shift frequency in the onshore area was 0.01 Hz. This could be due to low tide level of 0.3 m which was observed during in-situ data collection.

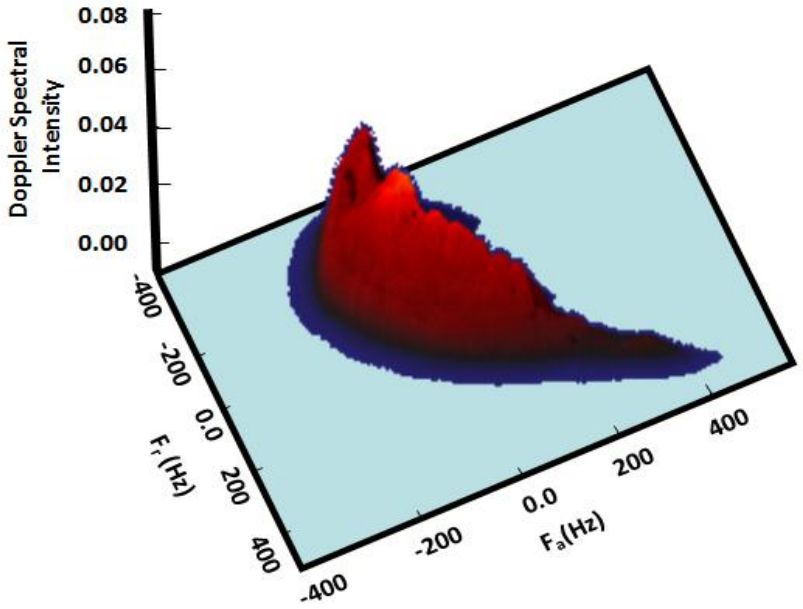

Figure 3. Doppler Spectra Intensity of TanDEM-X data

The TanDEM-X data with X-band of the spotlight product which derived from the strip-map mode has utilized in this study. The Figure 4 indicates the results that are retrieved from Hopfield rule and Pareto rule. It is attention-grabbing realize that Pareto algorithmic rule has found the most effective solution for sea surface current pattern as compared to Hopfield neural network (Figure 4b). The morphology of ocean surface current structures are well known exploitation Pareto algorithmic rule. Indeed, random generation of 1000 iterations at intervals 3 min are needed to realize the performance of the Pareto algorithmic program. Clearly, Pareto algorithm delivered a spatial variation of surface current from onshore to offshore. Onshore surface current is dominated by maximum value of 0.12 m/s while the offshore surface currents have maximum value of 0.2 m/s.

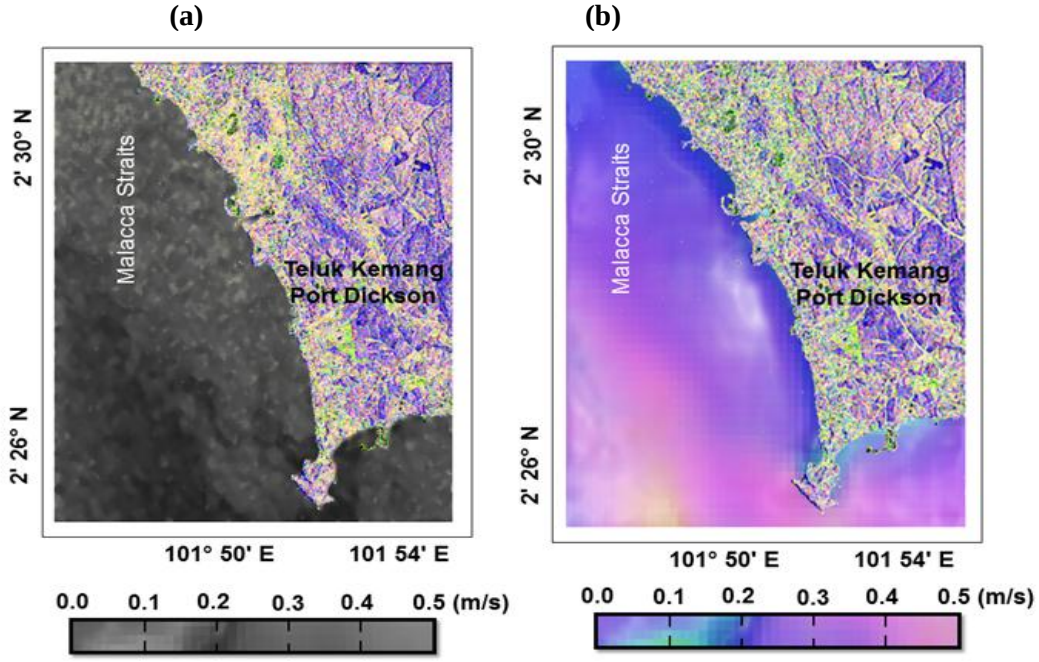

Figure 4. Ocean current pattern simulated from (a) Hopfield neural network result (b) Pareto optimal solution

Figure 5 shows significant correlations between the result of sea surface current velocities which simulated from TanDEM-X data and the result extracted in the *in-situ* measurement. Figure 5 illustrates how the correlation coefficient changes as the linear relationship between the two variables is altered. While in regression the emphasis is on predicting one variable from the other, in correlation the emphasis is on the degree to which a linear model may describe the relationship between two variables. Clearly, there is a good relationship between the two variables with R^2 of 0.75.

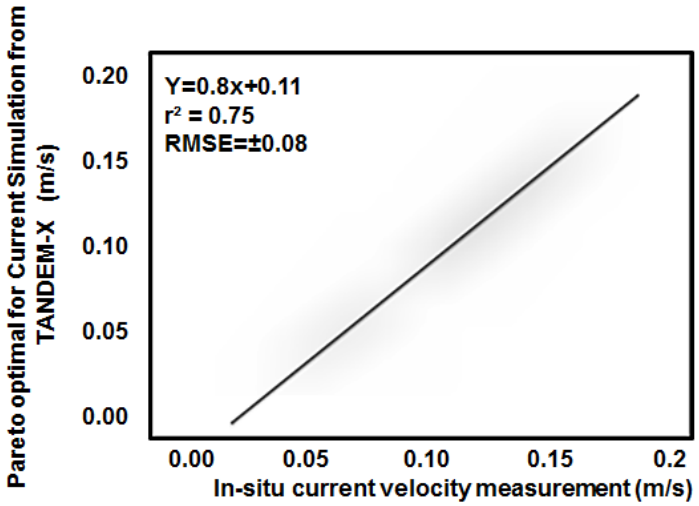

Figure 5. Significant correlation between Pareto Optimal and in situ measurements

However, this relationship is not perfect, but seems to have a positive linear relationship, and corresponds to what one would expect when considering two variables correlated and following the assumption of normality. Table 1 delivers the accuracy of this study. Clearly, the Pareto optimal solution has an excellent performance than Hopfield algorithm, with lowest *P* value of 0.00006 and RMSE of ±0.009 and highest r^2 of 0.75. Consistent with Marghany and Mansor [12] and Marghany [19], the Hopfield neural network is anticipated as optimization tool to reduce the impact of the Doppler nonlinearity in the SAR data. Subsequently, multi-objective optimization is fairly deliberated as attaining a vector of verdict variables satisfying constraints to offer precise to all objective functions. This confirms study of Marghany and Mansor [12].

Table 1. Statistical regression of current meter sea surface current and retrieved one by Hopfield neural network based Pareto optimal solution

Methods	R2	RMSE (±m/s)	***P***
Hopfield neural network-Current	0.55	0.2	0.00060
Pareto optimal solution-Current meter	0.75	0.08	0.000086

Additionally, the multi-objective optimisation via Pareto dominance acquires a particular curve that reduces the inconsistency between the certain ocean surface current from TanDEMX data and in situ measurements. In this understanding, the new approach supported TanDEMX data and as a result the multi-objective optimisation via Pareto Dominance, know how to minimalize the number of the residual faults for retrieving ocean surface current from TanDEMX data and delivers precise ocean surface current pattern spatial variation. This work recommends the work done by Atashkari et al., [22] and Marghany [19]. Moreover, it is suggested to exploit the time series of TanDEMX satellite data for watching the daily coastal current and its seasonal variations.

5. Conclusion

This work initiated a new approach for sea surface current studies along Malaysian coastal waters. This is first experimental operated TanDEM-X satellite not only in Malaysia but in all the South-east Asian coastal waters. Two approaches are prescribed: (i) Hopfield neural network rule; and (ii) Pareto optimum resolution. The study shows that the Pareto optimum resolution has highest performance than Hopfield neural network rule with lowest RMSE of ±0.08. Further, Pareto optimum resolution can verify the ocean surface current pattern variation using TanDEMX data. In conclusion, TanDEMX data reveals a superb guarantees for retrieving ocean surface current with X-band with VV polarization.

Acknowledgments
The author thanks the Geoinformation Global Space for using the high-performance programming facilities to build the code of Hopfield and Pareto algorithms.

References

[1] ALPERS, W.R., ROSS, D.B. AND RUFENACH, C.L., et.al. 1981, On the Detectability of Ocean Surface Waves by Real and Synthetic Aperture Radar[J]. *Journal of Geophysical Research: Oceans*, ***86***(C7): 6481-6498.

[2] ALPERS, W.R. AND BRUENING, C., et.al. 1986, On the Relative Importance of Motion-Related Contributions to the SAR Imaging Mechanism of Ocean Surface Waves[J]. *IEEE Transactions on Geoscience and Remote Sensing*, **6**:873-885.

[3] AMINI, A.A., CHEN, Y., CURWEN, R.W., MANI, V. AND SUN, J., et.al. 1998, Coupled B-Snake Grids and Constrained Thin-Plate Splines for Analysis of 2-D Tissue Deformations from Tagged MRI[J]. *IEEE Transactions on Medical Imaging*, ***17***(3):344-356.

[4] BEAL, R.C., TILLEY, D.G. AND MONALDO, F.M., et.al. 1983, Large-and Small-Scale Spatial Evolution of Digitally Processed Ocean Wave Spectra from SEASAT Synthetic Aperture radar[J]. *Journal of Geophysical Research: Oceans*, ***88***(C3):1761-1778.

[5] FORGET, P., BROCHE, P. AND CUQ, F., et. al. 1995, Principles of Swell Measurement by SAR with Application to ERS-1 Observations off the Mauritanian Coast[J]. *International Journal of Remote Sensing*, ***16***(13):.2403-2422.

[6] HERBERS, T.H.C., ELGAR, S. AND GUZA, R.T., et.al. 1999, Directional Spreading of Waves in the Nearshore{J]. *Journal of Geophysical Research: Oceans*, ***104***(C4):7683-7693.

[7] HASSELMANN, K. AND HASSELMANN, S., et.al. 1991. On the Nonlinear Mapping of an Ocean Wave Spectrum into a Synthetic Aperture Radar Image Spectrum and its Inversion[J]. *Journal of Geophysical Research: Oceans*, ***96***(C6):10713-10729.

[8] LI, X., LEHNER, S. AND ROSENTHAL, W., et.al.2010. Investigation of Ocean Surface Wave Refraction Using TerraSAR-X data[J]. *IEEE Transactions on Geoscience and Remote Sensing*, ***48***(2):830-840.

[9] MARGHANY, M.M., 2001, TOPSAR Wave Spectra Model and Coastal Erosion Detection[J]. *International journal of applied earth observation and geoinformation*, ***3***(4):357-365.

[10] MARGHANY, M., 2011, Developing Robust Model for Retrieving Sea Surface Current from RADARSAT-1 SAR Satellite Data[J]. *International Journal of Physical Sciences*, ***6***(29):6630-6637.

[11] MARGHANY ,M. 2015, Simulation Sea Surface Current from RADARSAT-2 SAR Data Using Hopfield Neural Network. In *Synthetic Aperture Radar (APSAR), 2015 IEEE 5th Asia-Pacific Conference on* (pp. 805-808). IEEE

[12] MARGHANY M and MANSOR S 2016 , Retrieving of Sea Surface Current Variations from Sentinel-1A Satellite Data. CD of 37th Asian Conference on Remote Sensing (ACRS), 37th ACRS from 17th - 21st October 2016, Galadari Hotel,Colombo,Sri Lanka,pp.1-6.

[13] ROMEISER, R. and RUNGE, H., 2007, Theoretical Evaluation of Several Possible Along-Track InSAR Modes of TerraSAR-X for Ocean Current Measurements[J] . *IEEE Transactions on Geoscience and Remote Sensing*, ***45***(1):21-35.

[14] ROMEISER, R., SUCHANDT, S., RUNGE, H., STEINBRECHER, U. and GRUNLER, S., et.al. 2010, First Analysis of TerraSAR-X Aong-Track InSAR-Derived Current Fields.[J] *IEEE Transactions on Geoscience and Remote Sensing*, ***48***(2):820-829.

[15] MARGHANY, M., 2009, Volterra–Lax-Wendroff Algorithm for Modelling Sea Surface Flow Pattern from Jason-1 Satellite Altimeter Data[J]. In *Transactions on Computational Science* **VI**:1-18.

[16] MARGHANY, M., 2011, Three-Dimensional Coastal Water Front Reconstruction from RADARSAT-1 Synthetic Aperture Radar (SAR) Satellite Data[J]. *International Journal of Physical Sciences*, ***6***(29): 6653-6659.

[17] MARGHANY M 2009, Robust Model for Retrieval Sea Surface Current from Different RADARSAT-1 SAR Mode Data. *Signal and Image Processing Applications (ICSIPA), 2009 IEEE International Conference on*, 2009, pp. 492-495.

[18] ROMEISER, R., RUNGE, H., SUCHANDT, S., KAHLE, R., ROSSI, C. AND BELL, P.S., 2014, Quality Assessment of Surface Current Fields From TerraSAR-X and TanDEM-X Along-Track Interferometry and Doppler Centroid Analysis[J]. *IEEE Transactions on Geoscience and Remote Sensing*, ***52***(5):2759-2772.

[19] MARGHANY M 2017 , Sea Surface Retrieving from TanDEM-X Satellite Data. *Proceedings of 38th Asian Conference on Remote Sensing (ACRS),New Delhi, India, www.a-a-r*s.org/acrs/administrator/components/com_jresearch/files/.../689.pdf [Acess on March 12 2018]

[20] COTE, S. and TATNALL, A.R.L., 1997, The Hopfield Neural Network as a Tool for Feature Tracking and Recognition from Satellite Sensor Images[J]. *International Journal of Remote Sensing*, ***18***(4):.871-885.

[21] CAO, J. and WANG, J., 2003, Global Asymptotic Stability of a General Class of Recurrent Neural Networks with Time-Varying Delays [J]. *IEEE Transactions on Circuits and Systems I: Fundamental Theory and Applications*, ***50***(1):34-44.

[22] ATASHKARI, K., NARIMAN-ZADEH, N., DARVIZEH, A., YAO, X., JAMALI, A. and PILECHI, A., 2004, Genetic Design of GMDH-Type Neural Networks for Modelling of Thermodynamically Pareto Optimized Turbojet Engines[J]. *WSEAS Transactions on Computers*, ***3***(3):719-724.